Journal of Coordination Chemistry

ISSN: 0095-8972 (Print) 1029-0389 (Online) Journal homepage: http://www.tandfonline.com/loi/gcoo20

Copper(I)-1,1,1-tris(diphenylphosphinomethyl)ethane complexes with different coordination modes tuned by auxiliary ligands and their spectroscopic properties

Zi-Cheng Fu, Qi Yin, Zu-Fu Yao, Cong Li & Wen-Fu Fu

To cite this article: Zi-Cheng Fu, Qi Yin, Zu-Fu Yao, Cong Li & Wen-Fu Fu (2015) Copper(I)-1,1,1-tris(diphenylphosphinomethyl)ethane complexes with different coordination modes tuned by auxiliary ligands and their spectroscopic properties, Journal of Coordination Chemistry, 68:17-18, 3282-3294, DOI: 10.1080/00958972.2015.1057507

To link to this article: http://dx.doi.org/10.1080/00958972.2015.1057507

Accepted author version posted online: 09 Jun 2015.
Published online: 30 Jun 2015.

Journal of Coordination Chemistry, 2015
Vol. 68, Nos. 17–18, 3282–3294, http://dx.doi.org/10.1080/00958972.2015.1057507

Copper(I)-1,1,1-tris(diphenylphosphinomethyl)ethane complexes with different coordination modes tuned by auxiliary ligands and their spectroscopic properties

ZI-CHENG FU†, QI YIN‡, ZU-FU YAO‡, CONG LI‡ and WEN-FU FU*†‡

†Technical Institute of Physics and Chemistry, Chinese Academy of Sciences, Beijing, PR China
‡College of Chemistry and Chemical Engineering, Yunnan Normal University, Kunming, PR China

(*Received 1 February 2015; accepted 23 April 2015*)

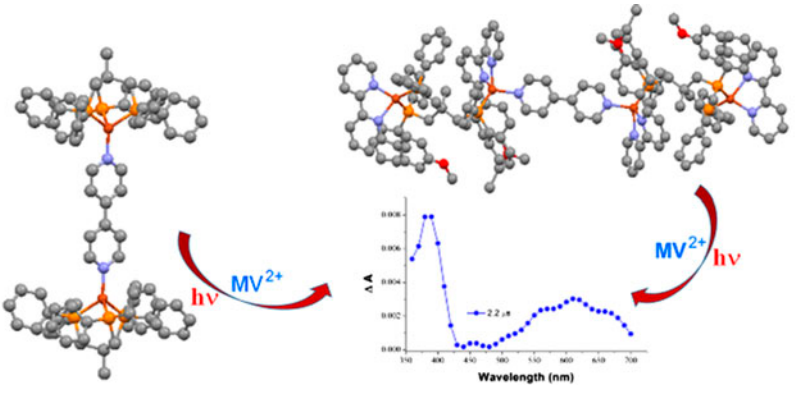

Three mono-, bi- and tetranuclear copper(I) complexes, [Cu(phen)(triphos-O)]BF_4 (**1**) (phen = 1,10-phenanthroline, triphos = 1,1,1-tris(diphenylphosphinomethyl)ethane), [Cu_2(bipy)(triphos)$_2$]$(BF_4)_2$ (**2**) (bipy = 4,4′-bipyridine), and [Cu_4(MeOC^N^N)$_4$(triphos)$_2$(bipy)]$(BF_4)_4$ (**3**) (MeOC^N^N = 6-(4-methoxyphenyl)-2,2′-bipyridine), have been synthesized and characterized by NMR spectroscopy, electrospray ionization, and matrix-assisted laser desorption ionization time-of-flight mass spectrometries, elemental analysis, and X-ray crystal analysis. The crystal structure investigation revealed the copper ions of the complexes have pseudo-tetrahedral coordination geometry. The electronic absorption spectra of **1**, **2,** and **3** contain low-energy bands at 350–500 and 400–650 nm, which are assigned to d(Cu) → π^*(phen or bipy) and a mixture of d(Cu) → π^*(MeOC^N^N) and d(Cu) → π^*(bipy) transitions, respectively. Complex **2** displays a strong, long-lived solid-state emission with a maximum at 555 nm and lifetime of 13.6 μs at room temperature. Photoinduced electron-transfer properties of **2** and **3** involving nanosecond time-resolved absorption spectroscopy and electron spin resonance techniques were studied.

Keywords: Copper(I) complexes; Triphos; Diimine; Crystal structure; Coordination model; Spectroscopic properties

*Corresponding author. Email: fuwf@mail.ipc.ac.cn

Dedicated to Professor Rudi van Eldik on the occasion of his 70th birthday.

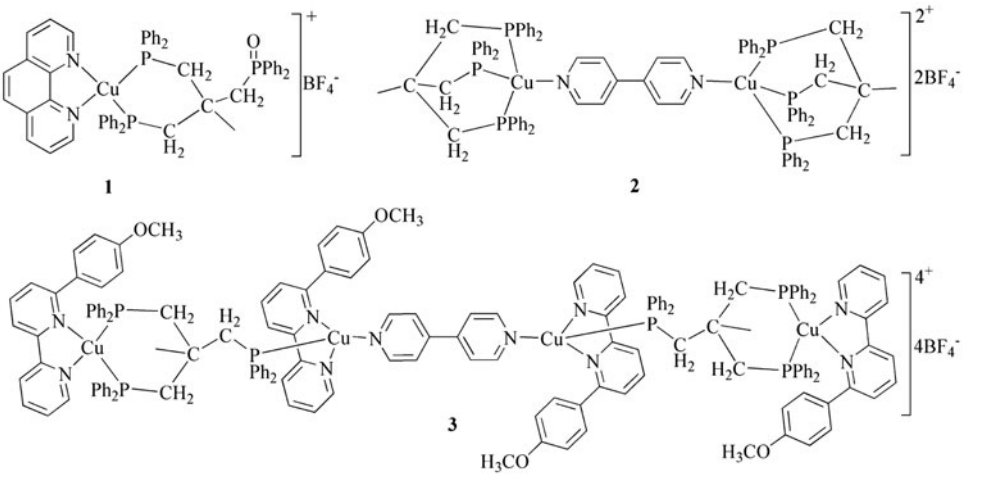

Scheme 1. The chemical structures of **1–3**.

1. Introduction

Copper(I) complexes containing aromatic diimine and/or phosphine ligands exhibit low-energy metal-to-ligand charge-transfer (MLCT) transitions and have been extensively studied because of their photophysical properties, photoinduced electron-transfer, and excited state substrate-binding reactions [1–9]. The steric and/or electronic effects of ligands in these complexes on excited state properties have been elaborated in the literature [10–17]. Although the photophysical properties of copper(I) complexes containing 1,10-phenanthroline (phen) have been comprehensively examined, few related studies on Cu(I) complexes containing substituted 2,2′-bipyridine, phosphine, and bipy bridging ligands have been reported [18–21]. Reaction of 1,1,1-tris(diphenylphosphinomethyl)ethane (triphos) as a tridentate phosphine ligand with CuX (X=Cl, Br) gave a closed monomeric complex with three six-membered rings [22–24]. The rigid structure prevents extensive excited state distortions and reduces radiationless deactivations, thereby resulting in an increase in emission quantum yield. Applications of inexpensive copper(I)-organic compounds as electroluminescent materials have been reported over the past decade [25, 26]. Subsequent research revealed that the reaction of mononuclear complexes [CuX(triphos)] and potassium thiolate generates [Cu(triphos)(thiolate)]. This complex exhibits intense blue-green emission, which is assigned to ligand–ligand charge transfer mediated by the copper(I) center [27]. In addition, Glueck and coworkers reported that a copper(I)-triphos complex with a diphenylphosphine auxiliary ligand can catalyze alkylation of diphenylphosphine [28]. Despite investigation of the coordination chemistry of different metals with triphos [29–31], research on copper(I) complexes containing a triphos ligand with κ^1 bonding, κ^2- and κ^3-chelating modes, and a diimine ligand is still inadequate. In this study, the synthesis and crystal structures of three copper(I) complexes, $[Cu(phen)(triphos\text{-}O)]BF_4$ (**1**), $[Cu_2(bipy)(triphos)_2](BF_4)_4$ (**2**), and $[Cu_4(MeOC\text{^}N\text{^}N)_4(triphos)_2(bipy)](BF_4)_4$ (**3**) (MeOC^N^N is 6-(4-methoxyphenyl)-2,2′-bipyridine) are presented (scheme 1) and their photophysical properties are described.

2. Experimental

2.1. *Materials and synthesis*

$[Cu(CH_3CN)_4]BF_4$ was prepared according to a published method [32]. 2-Acetylpyridine (Acros, 98%), triphos (Aldrich), and bipy (Acros, 98%) were used as received. All of the solvents obtained from commercial sources were purified and distilled by standard procedures prior to use. MeOC^N^N was synthesized according to the literature [19].

2.1.1. $[Cu(phen)(triphos\text{-}O)]BF_4$ (1). A mixture of $[Cu(CH_3CN)_4]BF_4$ (125.8 mg, 0.40 mmol) and phen (72.1 mg, 0.40 mmol) in dichloromethane (20 mL) was stirred for 3 h under a nitrogen atmosphere at room temperature. Triphos (249.9 mg, 0.40 mmol) was added and the mixture was stirred for a further 3 h. The resulting solution was then concentrated *in vacuo* and the crude product was precipitated by addition of diethyl ether. The solid was filtered and redissolved in the minimum volume of dichloromethane. Single crystals suitable for X-ray diffraction (XRD) were grown from a dichloromethane solution of the complex by vapor diffusion with diethyl ether. Yield 256.4 mg, 66%. ESI-MS: *m/z* 884.42 $[M–BF_4]^+$. Anal. Calcd for $C_{53}H_{47}BCuF_4N_2OP_3$: C, 65.54; H, 4.88; N, 2.88. Found: C, 65.36; H, 4.82; N, 2.96.

2.1.2. $[Cu_2(bipy)(triphos)_2](BF_4)_2$ (2) [25]. A mixture of $[Cu(CH_3CN)_4]BF_4$ (125.8 mg, 0.40 mmol) and triphos (249.9 mg, 0.40 mmol) in dichloromethane (20 mL) was stirred at room temperature for 3 h, followed by addition of bipy (47.1 mg, 0.30 mmol). The resulting yellow solution was stirred for 6 h and then filtered. The reaction mixture was concentrated *in vacuo* and then the crude product was recrystallized from dichloromethane/diethyl ether to give yellow crystals. Yield 259.3 mg, 76%. ESI-MS: *m/z* 766.31 $[M\text{-}2BF_4]^{2+}$. ^1H NMR (CD_2Cl_2, 300 MHz): 1.60 (s, 6H, Me), 2.55 (s, 12H, CH_2), 7.10 (t, $J = 7.3$ Hz, 24H, Ph), 7.22 (d, $J = 6.7$ Hz, 36H, Ph), 8.26 (d, $J = 6.1$ Hz, 4H, Py), 9.24 (d, $J = 5.8$ Hz, 4H, Py). Anal. Calcd for $C_{92}H_{86}B_2Cu_2F_8N_2P_6$: C, 64.76; H, 5.08; N, 1.64. Found: C, 64.84; H, 5.17; N, 1.75.

2.1.3. $[Cu_4(MeOC\text{^}N\text{^}N)_4(triphos)_2(bipy)](BF_4)_4$ (3). A mixture of $[Cu(CH_3CN)_4]BF_4$ (125.8 mg, 0.40 mmol)) and bipy (31.2 mg, 0.20 mmol) in dichloromethane (25 mL) was stirred at room temperature for 2 h under nitrogen. MeOC^N^N (110.2 mg, 0.42 mmol) in dichloromethane (5 mL) was then added dropwise to the solution, which changed from yellow to dark red. After stirring for 3 h, triphos (131.2 mg, 0.21 mmol) in dichloromethane (5 mL) was added to the reaction mixture. The resulting brown solution was stirred for 3 h. Evaporation of solvent followed by addition of diethyl ether afforded a brown precipitate. Recrystallization by slow diffusion of diethyl ether into a dichloromethane solution yielded brown crystals that were suitable for characterization by XRD. Yield 210.9 mg, 69%. TOF-MS: 2708.98. ^1H NMR (CD_2Cl_2, 300 MHz): 1.61 (s, 6H, Me), 2.55 (s, 12H, CH_2), 3.63 (s, 12H, OMe), 6.29 (d, $J = 8.0$ Hz, 8H), 7.10 (t, $J = 7.1$ Hz, 24H, Ph), 7.21 (d, $J = 6.9$ Hz, 36H, Ph), 7.27 (d, $J = 10.2$ Hz, 4H), 7.48–7.56 (m, 12H), 7.90 (d, $J = 7.0$ Hz, 8H), 8.06 (t, $J = 7.9$ Hz, 4H), 8.18 (d, $J = 8.0$ Hz, 4H), 8.26 (d, $J = 6.0$ Hz, 4H, Py), 8.47 (s, 4H), 9.24 (d, $J = 6.0$ Hz, 4H, Py). Anal. Calcd for $C_{160}H_{142}B_4Cu_4F_{16}N_{10}O_4P_6$: C, 62.88; H, 4.68; N, 4.58. Found: C, 62.97; H, 4.72; N, 4.51.

2.2. *Instrumentation and physical characterization*

Mass spectra were obtained on a Bruker BIFLEX III matrix-assisted laser desorption ionization time-of-flight (MALDI-TOF) and APEX II FT-ICR mass spectrometers. ^{1}H NMR spectra were recorded with a Bruker DRX 300 MHz resonance spectrometer with chemical shifts reported relative to tetramethylsilane. Elemental analyses were performed on a Vario EL III elemental analyzer. UV–vis absorption spectra were recorded using a Hitachi U-3010 spectrophotometer. Steady state emission spectra were measured on a Hitachi F-4500 fluorescence spectrophotometer. Flash photolysis was carried out on an Edinburgh Instruments LP900 spectrometer (pulse output 355 nm, 8 ns). Electron spin resonance (ESR) spectra were recorded using a Bruker ER046 X-band microwave bridge.

The amount of samples remaining did not allow to collect meaningful IR and ^{13}C-NMR data, and we plan to publish this later.

2.3. *Calculation details and X-ray crystallography*

Time-dependent density functional theory at the TD-DFT(B3LYP/6–311 + G*) level was also carried out with Gaussian 03 to predict and verify the absorption spectra of various species [33, 34]. Contour plots of molecular orbitals (MOs) were obtained with the Gauss View 3.07 program.

Crystals of **1–3** were obtained by slow diffusion of diethyl ether into dichloromethane solutions of the complexes over a period of several days. XRD measurements of single

Table 1. X-ray crystallographic data for **1–3**.

Complex	1	2	3
Formula	$C_{54}H_{49}BCl_2CuF_4N_2O_{0.50}P_3$	$C_{96}H_{94}B_2Cl_8Cu_2F_8N_2P_6$	$C_{162}H_{146}B_4Cl_4Cu_4F_{16}N_{10}O_4P_6$
M	1048.11	2045.85	3225.91
T (K)	293(2)	293(2)	293(2)
Crystal system	Triclinic	Monoclinic	Triclinic
Space group	*P-1*	*P2(1)/c*	*P-1*
a [Å]	10.350(3)	13.503(4)	12.307(4)
b [Å]	12,972(4)	17.666(6)	13.462(5)
c [Å]	21.556(6)	22.030(8)	24.306(9)
α [°]	105.257(5)	90	101.008(7)
β [°]	90.941(5)	109.768(14)	96.027(7)
γ [°]	98.107(5)	90	91.929(7)
V [Å^3]	2568.3(13)	4945(3)	3925(2)
Z	2	2	1
*D*c [g cm^{-3}]	1.355	1.374	1.365
Crystal size [mm]	0.20 × 0.16 × 0.12	0.22 × 0.20 × 0.18	0.24 × 0.14 × 0.12
F (0 0 0)	1080	2100	1658
Index range (*h*, *k*, *l*)	−12, 12; −9, 14; −25, 25	−16, 16; −21, 16; −25, 26	−14, 14; −13, 16; −28, 25
$2\theta_{max}$ [°]	50	50	50
Reflections collected/ unique	13,334/9016	23,475/8575	20,302/13,700
*R*1, *wR*2 [$I > 2\sigma(I)$][a]	0.0531, 0.1289	0.0629, 0.1686	0.0641, 0.1529
*R*1, *wR*2 (all data)	0.0944, 0.1621	0.1049, 0.1996	0.1463, 0.1989
Goodness of fit	1.007	1.036	1.020
Residual electron density [e Å^{-3}]	0.466, −0.366	0.828, −0.902	0.803, −0.332

[a] $R_1 = \sum ||F_o| - |F_c|| \sum |F_o|. wR_2 = \left\{ \sum \left[w(F_o^2 - F_c^2)^2 \right] / \sum \left[w(F_o^2)^2 \right] \right\}^{\frac{1}{2}}$.

crystals of **1–3** were carried out on a Bruker SMART diffractometer using a graphite monochromator with Mo-Kα radiation (λ = 0.071073 nm) at room temperature. An absorption correction was applied by correction of symmetry-equivalent reflections using the ABSCOR program. The structures of the complexes were solved by direct methods using SHELXS-97 software [35, 36]. All non-hydrogen atoms were refined anisotropically by full-matrix least-squares using F^2 data. The crystallographic parameters and data are summarized in table 1.

3. Results and discussion

3.1. *Structure descriptions*

The XRD analysis of mononuclear **1** revealed that the complex contains an uncoordinated phosphorus and it is curious that one of the seemingly equivalent phosphorus atoms was oxidized to form a P–O bond with length of 1.348(1) Å (figure 1 and table 2), which indicates that the free phosphorus in triphos is unstable and oxidized in the experimental process. The two other phosphorus atoms of triphos bind to copper(I) in a bidentate fashion to form one six-membered ring with an average Cu–P bond length of 2.251 Å and P(2)–Cu(1)–P(1) angle of 100.58(5)°. Meanwhile, phen adopted its usual chelating mode with an average Cu–N distance of 2.075(4) Å and N(1)–Cu(1)–N(2) angle of 80.9(1)° in the resulting five-membered chelate ring. The coordination geometry of the copper(I) center is distorted tetrahedral; selected bond lengths and angles for **1** are listed in table 2.

Reaction of a suspension of $[Cu(CH_3CN)_4]BF_4$, bipy, and triphos with a 1 : 0.75 : 1 M ratio in dichloromethane under nitrogen afforded **2** as a yellow solid upon precipitation by diethyl ether. The structure of **2** determined by XRD analysis is a centrosymmetric dinuclear complex (figure 2) and is similar to that of $[Cu_2(4,4'\text{-azbpy})(triphos)_2](BF_4)_2$ (azbpy = azobipyridine) reported by our group [37]. Each copper(I) in the complex has a closed κ^3-coordinated triphos and adopts a distorted tetrahedral coordination geometry with Cu–P distances of 2.288(1)–2.306(2) Å. The major distortion of the tetrahedral geometry arises from the P–Cu(1)–P bond angles that range from 93.74(5)° to 95.91(5)° and average N(1)–Cu(1)–P bond angle of 121.8(1)°. The two P_3Cu^+ fragments are ligated together by a bridging bipy ligand with an intrametallic Cu···Cu distance of 11.202 Å.

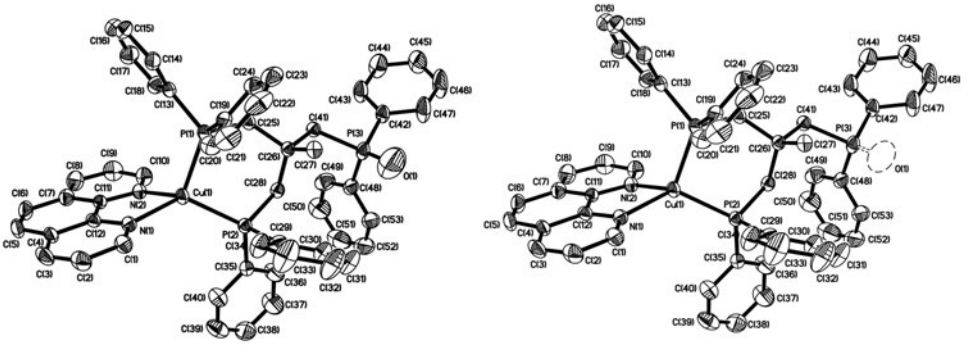

Figure 1. The perspective view and labeling scheme for the cation of **1**. The anion and hydrogens are omitted for clarity.

Table 2. Selected bond lengths and angles of **1–3**.

Complex **1**			
Cu(1)–N(1)	2.072(3)	Cu(1)–N(2)	2.077(4)
Cu(1)–P(1)	2.264(1)	Cu(1)–P(2)	2.237(1)
P(3)–C(41)	1.846(4)	P(3)–C(42)	1.829(5)
P(3)–C(48)	1.824(6)	P(3)–O(1)	1.348(1)
N(1)–Cu(1)–N(2)	80.9(1)	N(1)–Cu(1)–P(2)	124.9(1)
N(2)–Cu(1)–P(2)	119.7(1)	N(1)–Cu(1)–P(1)	122.6(1)
N(2)–Cu(1)–P(1)	107.1(1)	P(2)–Cu(1)–P(1)	100.58(5)
O(1)–P(3)–C(48)	113.3(7)	O(1)–P(3)–C(42)	112.3(7)
O(1)–P(3)–C(41)	120.6(6)	C(27)–C(26)–C(28)	112.3(4)
C(28)–C(26)–C(41)	106.7(3)	C(25)–C(26)–C(41)	103.9(3)
Complex **2**			
Cu(1)–N(1)	2.030(4)	Cu(1)–P(1)	2.306(2)
Cu(1)–P(2)	2.288(1)	Cu(1)–P(3)	2.299(1)
N(1)–Cu(1)–P(2)	125.0(1)	N(1)–Cu(1)–P(3)	119.4(1)
P(2)–Cu(1)–P(3)	93.74(5)	N(1)–Cu(1)–P(1)	121.2(1)
P(2)–Cu(1)–P(1)	94.58(5)	P(3)–Cu(1)–P(1)	95.91(5)
C(42)–N(1)–Cu(1)	122.5(3)	C(46)–N(1)–Cu(1)	122.7(3)
Complex **3**			
Cu(1)–N(1)	2.021(5)	Cu(1)–N(2)	2.217(5)
Cu(1)–P(1)	2.229(2)	Cu(1)–P(2)	2.240(2)
Cu(2)–N(3)	2.087(5)	Cu(2)–N(5)	2.124(5)
Cu(2)–N(4)	2.139(6)	Cu(2)–P(3)	2.214(2)
N(1)–Cu(1)–N(2)	79.4(2)	N(1)–Cu(1)–P(1)	131.1(2)
N(2)–Cu(1)–P(1)	99.9 (1)	N(1)–Cu(1)–P(2)	117.6(2)
N(2)–Cu(1)–P(2)	127.5(1)	P(1)–Cu(1)–P(2)	101.47(6)
N(3)–Cu(2)–N(5)	98.8(2)	N(3)–Cu(2)–N(4)	78.7(2)
N(5)–Cu(2)–N(4)	106.8(2)	N(3)–Cu(2)–P(3)	127.1(2)
N(5)–Cu(2)–P(3)	116.8(2)	N(4)–Cu(2)–P(3)	121.4(1)
C(35)–N(5)–Cu(2)	123.0(4)	C(39)–N(5)–Cu(2)	121.3(4)

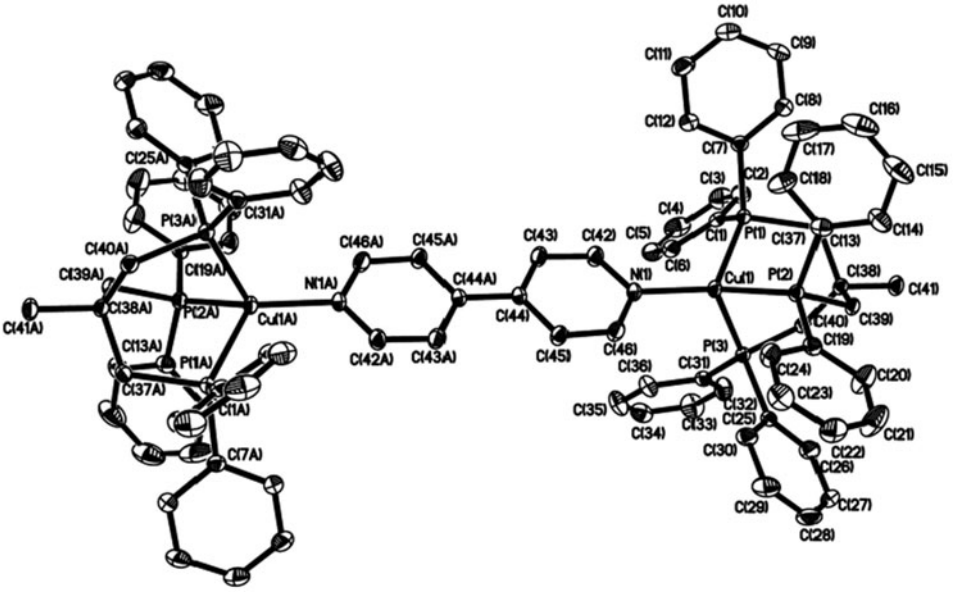

Figure 2. The perspective view and labeling scheme for the cation of **2**. The anion and hydrogens are omitted for clarity.

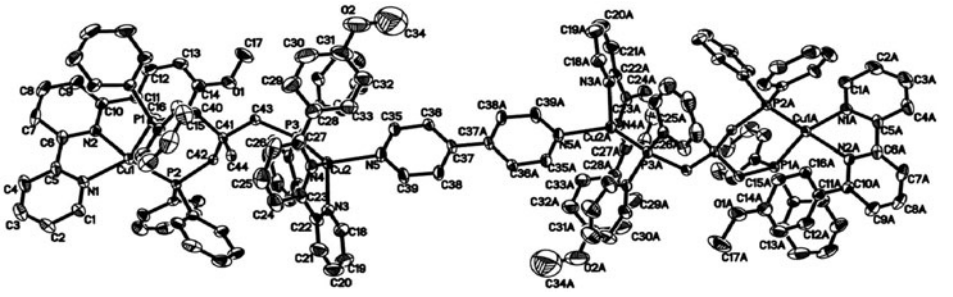

Figure 3. The perspective view and labeling scheme for the cation of **3**. The anion and hydrogens are omitted for clarity.

The XRD analysis of **3** (figure 3) revealed a tetranuclear framework where each copper unit is chelated to a MeOC^N^N ligand. The Cu–N bond lengths varying from 2.021 to 2.217 Å fall within the range of typical copper(I) complexes with the structure [Cu(substituted 2,2′-diimine)$_2$]$^+$ [38, 39]. There are two types of coordination environment around copper, $[P_2CuN_2]^+$ and $[PCuN_3]^+$. These two moieties are connected by a bridging triphos ligand in κ^2-chelating and κ^1-bonding modes, while $[N_2CuP_3CuN_2]^{2+}$ is held together through the nitrogens of a bridging bipy to yield a centrosymmetric tetranuclear complex.

The coordinated bipy bridging ligand of **3** is coplanar, whereas the coordinated 2,2′-bipyridine fragments of MeOC^N^N are not coplanar, with dihedral angles of 31.8° for Cu(1) and 39.4° for Cu(2) centers. These angles are much larger than those of 30.8° and 25.1° between the terminal aromatic ring and adjacent pyridine ring for Cu(1) and Cu(2), respectively. The intramolecular Cu···Cu distances are long: 7.715 Å for Cu(1)···Cu(2), 11.337 Å for Cu(2)···Cu(2A), 18.947 Å for Cu(1)···Cu(2A), and 26.618 Å for Cu(1)···Cu(1A). No interaction between the BF_4^- and copper(I) is observed.

Table 3. Spectroscopic and photophysical properties of **1–3**.

Complex	Medium (*T*/*K*)	λ_{abs} (nm) (ε/M^{-1} cm^{-1})	λ_{em} (nm) (τ ns)	λ_{abs} (nm) (τ ns)
1	CH_3CN (298)	410 (1461)	Non-emissive	
	CH_2Cl_2 (298)	410 (5290)	Non-emissive	
	Solid (298)		580 (12.1)	
2	CH_2Cl_2 (298)	365 (7237)	Non-emissive	420 (62)
				550 (70)
				730 (70)
	$(CH_3)_2CO$ (298)		Non-emissive	530 (44)
				580 (43)
	Solid (298)		555 (13.6)	
	Solid (77)		580 (592)	
3	CH_2Cl_2 (298)	320 (sh, 52,031)	Non-emissive	440 (28, 238)
		420 (7808)		550 (34, 266)
		540 (3832)		730 (22, 254)
	$(CH_3)_2CO$ (298)		400 (0.058)	580 (54, 680)
				730 (84)

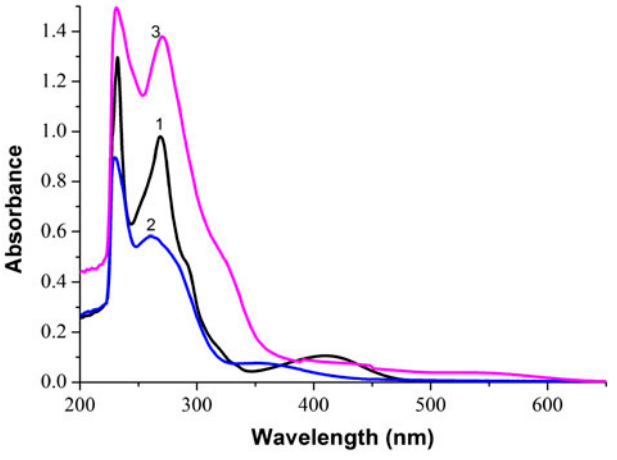

Figure 4. The electronic absorption spectra of **1–3** in dichloromethane at room temperature.

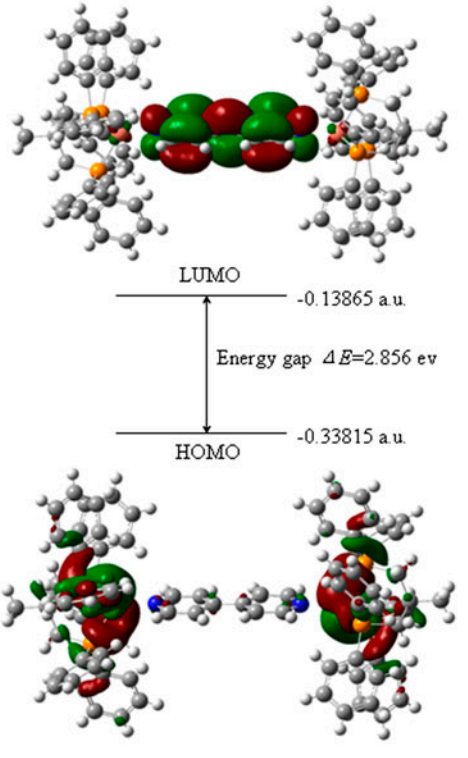

Figure 5. Contour plots and orbital energies of the HOMO and LUMO for **2**.

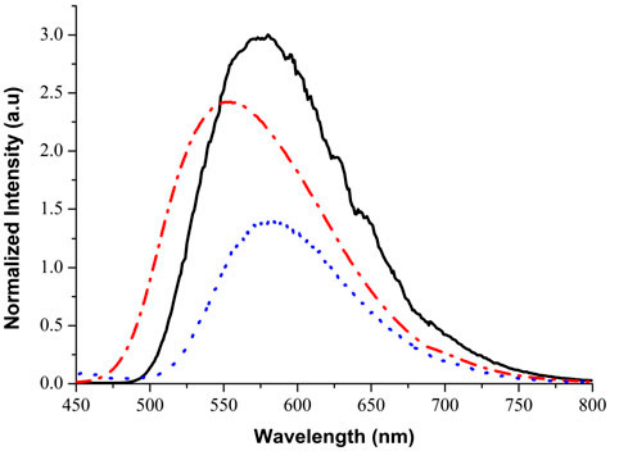

Figure 6. Room-temperature solid-state emission spectra of **1** (dotted line) and **2** (dash dot line) and the solid-state emission for **2** at 77 K (solid line) upon excitation at 360 nm.

3.2. *Electronic absorption spectroscopy and photoluminescence*

The UV–vis absorption spectral data of the copper(I) complexes in dichloromethane and acetonitrile solutions at room temperature are summarized in table 3 and depicted in figure 4. The intense peaks with absorption maxima (λ_{max}) < 280 nm are assigned to intraligand (IL) $\pi \rightarrow \pi^*$ transitions. The absorption at 320–450 nm is attributed to a MLCT 3d(Cu) $\rightarrow \pi^*$ (bipy) transition. Complex **1** exhibits an absorption at 410 nm that originates from a 3d (Cu) $\rightarrow \pi^*$(phen) transition. However, λ_{max} of **2** at 365 nm observed in dichloromethane is replaced by a long-wavelength tail extending beyond 530 nm in acetonitrile, indicating that **2** is unstable in acetonitrile. Unlike **2**, **3** shows low-energy absorptions at 420 and 540 nm with a tail extending to 700 nm in dichloromethane at room temperature, similar to the behavior of $[Cu(MeO\text{-}C\hat{}N\hat{}N)_2]BF_4$ and $[Cu_2(MeO\text{-}C\hat{}N\hat{}N)_2(PCy_3)_2(4,4'\text{-azpy})](BF_4)_2$ (PCy_3 = tricyclohexylphosphine) [19]. These low-energy visible absorption bands are therefore tentatively assigned to 3d(Cu)$\rightarrow\pi^*$(MeOC^N^N) transitions. A density functional theory calculation of **2** agreed with experimental data for the MLCT transition. The contour plot containing the highest occupied MO (HOMO) and lowest unoccupied MO (LUMO) together with the orbital energies (figure 5) demonstrates that the HOMO is mainly localized on central copper(I) d orbitals, while the LUMO displays the π^* character of bipy [40]. The energy gap between the HOMO and LUMO is 434 nm. Upon excitation at 360 nm at room temperature, **1** displays a moderate solid-state emission at 580 nm. Meanwhile, **2** exhibits an intense long-lived emission with λ_{max} at 555 nm (lifetime (τ) = 13.6 μs) in the solid state at room temperature and at 580 nm (τ = 592 μs) at 77 K (figure 6) [25], whereas **3** is non-emissive. The solid-state emissions of **1** and **2** can be attributed to the triplet 3d(Cu) $\rightarrow \pi^*$(diimine) excited state. However, **1** and **2** do not emit in degassed solutions of methanol, dichloromethane, acetonitrile, or acetone. In contrast, **3** exhibited weak room-temperature emission in acetone.

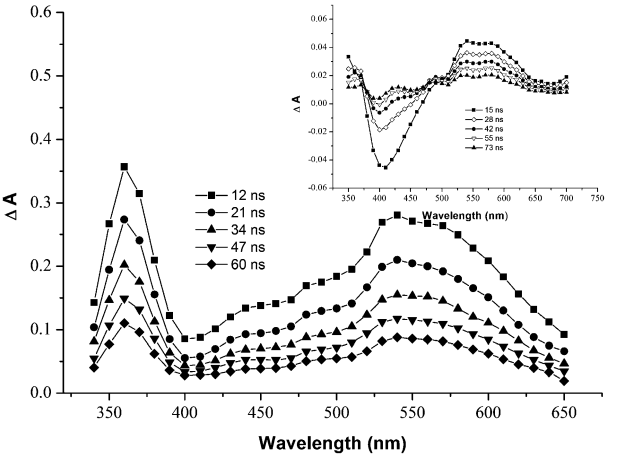

Figure 7. Room-temperature time-resolved difference absorption spectra of **2** (3.0×10^{-5} M) and **3** (6.0×10^{-5} M, inset) recorded at 150 ns after excitation at 355 nm in degassed acetone.

3.3. *Transient absorption spectra and photoinduced electron-transfer*

The transient absorption spectra of **2** and **3** were measured upon nanosecond-pulsed excitation at 355 nm in degassed acetone and dichloromethane. Both complexes in degassed acetone exhibit an intense absorption at 530–580 nm with τ of about 50 ns (figure 7 and table 3). These lifetimes match that of **3** in acetone solution, suggesting that the absorption and emission signals originate from the same excited state. By considering the structures of **2** and **3**, it was supposed that the absorption at 580 nm probably originates from

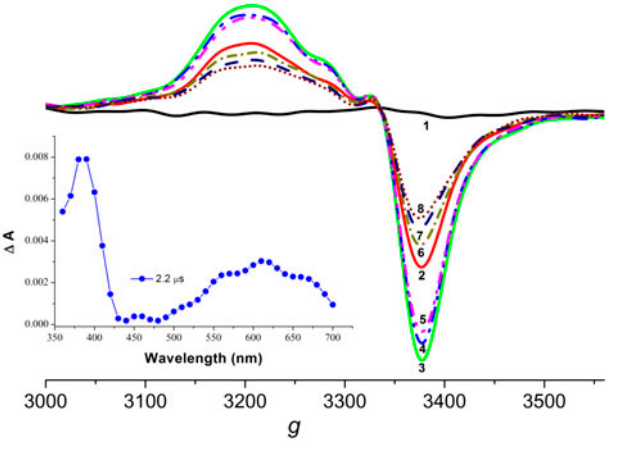

Figure 8. ESR spectral changes for **3** in dichloromethane upon light irradiation at 355 nm followed by the absence of light at room temperature. Original solution (curve 1); after irradiation for 4 min (curve 2); solution was kept in the dark for 4 min (curve 3), 8 min (curve 4), 16 min (curve 5), 80 min (curve 6), 100 min (curve 7), and 120 min (curve 8). Inset: room temperature time-resolved difference absorption spectra recorded at 5 μs after excitation at 355 nm for **3** and MV^{2+} in degassed acetonitrile.

Cu^{II}(diimine$^{\bullet-}$) species [41–43]. Excitation of degassed dichloromethane solutions of **2** and **3** gave similar absorption difference spectra except that **3** exhibits an intense absorption at 430 nm. In addition, the decays of absorption monitored at 420–730 nm for **2** in acetone and dichloromethane fit a first-order model, whereas those of **3** follow second-order kinetics. This indicates that for **3,** a new species might be generated at longer irradiation times [44].

To provide insight into the photophysical properties of the complexes, a room-temperature time-resolved difference absorption spectrum for **3** and methyl viologen (MV^{2+}) in degassed acetonitrile was measured following excitation at 355 nm. The characteristic absorption at 605 nm demonstrates the formation of $MV^{+\bullet}$ species by intermolecular photoinduced electron transfer (figure 8). Furthermore, we investigated photoinduced electron-transfer reactions of the complexes in dichloromethane at ambient temperature by ESR [45]. Upon irradiation of **3** at 355 nm, ESR signals at 3200–3400 G appeared, indicating the formation of copper(II) species in dichloromethane (figure 8) [46, 47]. No noticeable reaction was observed in acetonitrile or DMSO. Formation of copper(II) species from the reaction of copper(I) complexes with benzyl halides or in the presence of dichloromethane or chloroform has previously been observed [48, 49]. It is intriguing that the intensity of the ESR signals at 3200–3400 G increased continually and reached maxima when the irradiated sample was kept in the dark, and then subsequent decay was observed over a period of 120 min in the absence of light. A similar result was also found for **2**. Based on the ESR studies, it is tentatively suggested that upon excitation of the copper(I) complexes into the MLCT state, the electron density is shifted from the copper(I) center to bipy and geometric configuration changes of complex from tetrahedron to quadrangle occur, which may enable attack of the metal site by dichloromethane via formation of a $Cu^{+}\cdots Cl\cdots CH_2Cl$ intermediate. In the absence of light, the photoinduced generation of copper(II) species could be restored to initial Cu(I) state. However, we were unable to separate the product and obtain structural evidence of formation of a copper(II)–Cl complex in these systems.

4. Conclusion

Different diimine ligands were used to tune the structures of copper(I)-triphos complexes. The tripodal phosphine ligand in the obtained copper(I) complexes adopts chelating or bridging coordination modes depending on the diimine ligand. Nanosecond time-resolved absorption spectroscopy of the complexes indicated that the intense transient absorption band from 530 to 580 nm originates from d(Cu) $\rightarrow \pi^*$(diimine) excited states. ESR measurements of **2** and **3** in dichloromethane suggested that a copper(II) species is generated upon light excitation. Furthermore, an intermolecular photoinduced electron-transfer reaction occurred between MV^{2+} and these copper(I) complexes.

Supplementary material

Crystallographic data for the structures reported in this paper have been deposited with the Cambridge Crystallographic Data Centre as supplementary publication nos. CCDC-1046449 (**1**), CCDC-282479 (**2**), CCDC-282480 (**3**). These data can be obtained free of charge via www.ccdc.cam.ac.uk/conts/retrieving.htlm (or from the Cambridge Crystallographic Data

Centre, 12 Union Road, Cambridge CB2 1EZ, UK (Fax: (+44) 1223-336-033; or E-mail: deposit@ccdc.cam.ac.uk).

Disclosure statement

No potential conflict of interest was reported by the authors.

Funding

The work was supported by the National Natural Science Foundation of China (NSFC) [grant number 21267025], [grant number 21471155] and the foundation (2012DFH40090) for Bureau of International Co-operation of Chinese Academy of Sciences and Chunhui projects (Z2012050) of Chinese Ministry of Education.

References

[1] P.C. Ford, E. Cariati, J. Bourassa. *Chem. Rev.*, **99**, 3625 (1999).
[2] V.W.W. Yam, K.K.W. Lo. *Chem. Soc. Rev.*, **28**, 323 (1999).
[3] Z. Mao, H.-Y. Chao, Z. Hui, C.-M. Che, W.-F. Fu, K.-K. Cheung, N. Zhu. *Chem. Eur. J.*, **9**, 2885 (2003).
[4] L.X. Chen, G.B. Shaw, I. Novozhilova, T. Liu, G. Jennings, K. Attenkofer, G.J. Meyer, P. Coppens. *J. Am. Chem. Soc.*, **125**, 7022 (2003).
[5] M.A. Carvajal, S. Alvarez, J.J. Novoa. *Chem. Eur. J.*, **10**, 2117 (2004).
[6] M.S. Balakrishna, D. Suresh, A. Rai, J.T. Mague, D. Panda. *Inorg. Chem.*, **49**, 8790 (2010).
[7] P. Papanikolaou, J. Mohanraj, A. Czapik, M. Gdaniec, G. Accorsi, P. Akrivos. *Dalton Trans.*, **42**, 3357 (2013).
[8] X.-L. Xin, M. Chen, Y.-B. Ai, F.-L. Yang, X.-L. Li, F.-Y. Li. *Inorg. Chem.*, **53**, 2922 (2014).
[9] B. Wang, D. Prakash Shelar, X.-Z. Han, T.T. Li, X.G. Guan, W. Lu, K. Liu, Y. Chen, W.-F. Fu, C.-M. Che. *Chem. Eur. J.*, **21**, 1184 (2015).
[10] D.R. McMillin, K.M. McNett. *Chem. Rev.*, **98**, 1201 (1998).
[11] W.-F. Fu, X. Gan, C.-M. Che, Q.-Y. Cao, Z.-Y. Zhou, N.N.-Y. Zhu. *Chem. Eur. J.*, **10**, 2228 (2004).
[12] S. Hu, J.-C. Chen, M.-L. Tong, B. Wang, Y.-X. Yan, S.R. Batten. *Angew. Chem. Int. Ed.*, **44**, 5471 (2005).
[13] Y. Pellegrin, M. Sandroni, E. Blart, A. Planchat, M. Evain, N.C. Bera, M. Kayanuma, M. Sliwa, M. Rebarz, O. Poizat, C. Daniel, F. Odobel. *Inorg. Chem.*, **50**, 11309 (2011).
[14] M.G. Fraser, H. van der Salm, S.A. Cameron, A.G. Blackman, K.C. Gordon. *Inorg. Chem.*, **52**, 2980 (2013).
[15] S.-P. Luo, E. Mejía, A. Friedrich, A. Pazidis, H. Junge, A.-E. Surkus, R. Jackstell, S. Denurra, S. Gladiali, S. Lochbrunner, M. Beller. *Angew. Chem. Int. Ed.*, **52**, 419 (2013).
[16] C. Bizzarri, C. Strabler, J. Prock, B. Trettenbrein, M. Ruggenthaler, C.-H. Yang, F. Polo, A. Iordache, P. Brüggeller, L. De Cola. *Inorg. Chem.*, **53**, 10944 (2014).
[17] M.W. Mara, K.A. Fransted, L.X. Chen. *Coord. Chem. Rev.*, **282–283**, 2 (2015).
[18] R.M. Williams, L. De Cola, F. Hartl, J.-J. Lagref, J.-M. Planeix, A. De Cian, M.W. Hosseini. *Coord. Chem. Rev.*, **230**, 253 (2002).
[19] W.-F. Fu, X. Gan, J. Jiao, Y. Chen, M. Yuan, S.-M. Chi, M.-M. Yu, S.X. Xiong. *Inorg. Chim. Acta*, **360**, 2758 (2007).
[20] X. Gan, Z.-F. Yao, J.F. Zhang, Z. Li, W.-F. Fu. *J. Coord. Chem.*, **63**, 2800 (2010).
[21] W.-F. Fu, L.-F. Jia, W.H. Mu, X. Gan, J.-B. Zhang, P.-H. Liu, Q.-Y. Cao, G.-J. Zhang, L. Quan, X.-J. Lv, Q.-Q. Xu. *Inorg. Chem.*, **49**, 4254 (2010).
[22] A.B. Chaplin, P.J. Dyson. *Eur. J. Inorg. Chem.*, **31**, 4973 (2007).
[23] D.J. Fife, H.J. Mueh, C.F. Campana. *Acta Crystallogr., Sect. C: Crys. Struct. Commun.*, **49**, 1714 (1993).
[24] I. Warad, O.H. Abd-Elkader, A. Boshaala, N. Al-Zaqri, B. Hammouti, T.B. Hadda. *Res. Chem. Intermed.*, **39**, 721 (2013).
[25] Y.M. Wang, F. Teng, Y.B. Hou, Z. Xu, Y.S. Wang, W.-F. Fu. *Appl. Phys. Lett.*, **87**, 233512 (2005).
[26] V. Pawlowski, G. Knör, C. Lennartz, A. Vogler. *Eur. J. Inorg. Chem.*, **15**, 3167 (2005).
[27] P. Aslanidis, P.J. Cox, K. Kapetangiannis, A.C. Tsipis. *Eur. J. Inorg. Chem.*, **32**, 5029 (2008).
[28] M.F. Cain, R.P. Hughes, D.S. Glueck, J.A. Golen, C.E. Moore, A.L. Rheingold. *Inorg. Chem.*, **49**, 7650 (2010).
[29] A. Bencini, C. Benelli, D. Gatteschi, L. Sacconi. *Inorg. Chim. Acta*, **37**, 195 (1979).
[30] M.I. García-Seijo, P. Sevillano, R.O. Gould, D. Fernández-Anca, M.E. García-Fernández. *Inorg. Chim. Acta*, **353**, 206 (2003).

[31] H.J. Gysling, L.J. Gerenser, M.G. Mason. *J. Coord. Chem.*, **10**, 67 (1980).
[32] G.J. Kubas. *Inorg. Synth.*, **28**, 68 (1990).
[33] M.J. Frisch, G.W. Trucks, H.B. Schlegel, G.E. Scuseria, M.A. Robb, J.R. Cheeseman, J.A. Montgomery Jr., T. Vreven, K.N. Kudin, J.C. Burant, J.M. Millam, S.S. Iyengar, J. Tomasi, V. Barone, B. Mennucci, M. Cossi, G. Scalmani, N. Rega, G.A. Petersson, H. Nakatsuji, M. Hada, M. Ehara, K. Toyota, R. Fukuda, J. Hasegawa, M. Ishida, T. Nakajima, Y. Honda, O. Kitao, H. Nakai, M. Klene, X. Li, J.E. Knox, H.P. Hratchian, J.B. Cross, V. Bakken, C. Adamo, J. Jaramillo, R. Gomperts, R.E. Stratmann, O. Yazyev, A.J. Austin, R. Cammi, C. Pomelli, J.W. Ochterski, P.Y. Ayala, K. Morokuma, G.A. Voth, P. Salvador, J.J. Dannenberg, V.G. Zakrzewski, S. Dapprich, A.D. Daniels, M.C. Strain, O. Farkas, D.K. Malick, A.D. Rabuck, K. Raghavachari, J.B. Foresman, J.V. Ortiz, Q. Cui, A.G. Baboul, S. Clifford, J. Cioslowski, B.B. Stefanov, G. Liu, A. Liashenko, P. Piskorz, I. Komaromi, R.L. Martin, D.J. Fox, T. Keith, M.A. Al-Laham, C.Y. Peng, A. Nanayakkara, M. Challacombe, P.M.W. Gill, B. Johnson, W. Chen, M.W. Wong, C. Gonzalez, J.A. Pople, Gaussian 03, Revision C.01; Gaussian, Inc.; Wallingford, CT (2004).
[34] C. Lee, W. Yang, R.G. Parr. *Phys. Rev. B*, **37**, 785 (1988).
[35] G.M. Sheldrick. *SHELXS 97, Program for the Solution of Crystal Structure*, University of Göttingen, Germany (1997).
[36] G.M. Sheldrick. *SHELXL97, Program for the Refinement of Crystal Structures*, University of Göttingen, Germany (1997).
[37] M.M. Yu, Z.X. Li, W.F. Fu, J.F. Zhang. *Acta Crystallogr. Sect. E: Struct. Rep. Online*, **61**, m98 (2005).
[38] A.T. Levy, M.M. Olmstead, T.E. Patten. *Inorg. Chem.*, **39**, 1628 (2000).
[39] D.G. Cuttell, S.M. Kuang, P.E. Fanwick, D.R. McMillin, R.A. Walton. *J. Am. Chem. Soc.*, **124**, 6 (2002).
[40] M. Nishikawa, S. Sawamura, A. Haraguchi, J. Morikubo, K. Takao, T. Tsubomura. *Dalton Trans.*, **44**, 411 (2015).
[41] P. Lainé, F. Bedioui, E. Amouyal, V. Albin, F. Berruyer-Penaud. *Chem. Eur. J.*, **8**, 3162 (2002).
[42] S. Chakraborty, T.J. Wadas, H. Hester, R. Schmehl, R. Eisenberg. *Inorg. Chem.*, **44**, 6865 (2005).
[43] M. Nishikawa, K. Nomoto, S. Kume, H. Nishihara. *J. Am. Chem. Soc.*, **134**, 10543 (2012).
[44] C.M. Jones, M.J. Burkitt. *J. Am. Chem. Soc.*, **125**, 6846 (2003).
[45] J. Huang, O. Buyukcakir, M.W. Mara, A. Coskun, N.M. Dimitrijevic, G. Barin, O.C. He, S.J. Lippard. *Inorg. Chem.*, **39**, 5225 (2000).
[46] G. Kickelbick, U. Reinöhl, T.S. Ertel, A. Weber, H. Bertagnolli, K. Matyjaszewski. *Inorg. Chem.*, **40**, 6 (2001).
[47] J. Huang, O. Buyukcakir, M.W. Mara, A. Coskun, N.M. Dimitrijevic, G. Barin, O. Kokhan, A.B. Stickrath, R. Ruppert, D.M. Tiede, J.F. Stoddart, J.-P. Sauvage, L.X. Chen. *Angew. Chem. Int. Ed.*, **51**, 12711 (2012).
[48] Z. Tyeklar, R.R. Jacobson, N. Wei, N.N. Murthy, J. Zubieta, K.D. Karlin. *J. Am. Chem. Soc.*, **115**, 2677 (1993).
[49] T. Osako, K.D. Karlin, S. Itoh. *Inorg. Chem.*, **44**, 410 (2005).